Superplastic Behavior and Microstructure Evolution in a Commercial Al-Mg-Sc Alloy Subjected to Intense Plastic Straining

F. MUSIN, R. KAIBYSHEV, Y. MOTOHASHI, and G. ITOH

A commercial Al-6 pct Mg-0.3 pct Sc-0.3 pct Mn alloy subjected to equal-channel angular extrusion (ECAE) at 325 °C to a total strain of about 16 resulted in an average grain size of about 1 μm. Superplastic properties and microstructural evolution of the alloy were studied in tension at strain rates ranging from 1.4×10^{-5} to $1.4\ s^{-1}$ in the temperature interval 250 °C to 500 °C. It was shown that this alloy exhibited superior superplastic properties in the wide temperature range 250 °C to 500 °C at strain rates higher than $10^{-2}\ s^{-1}$. The highest elongation to failure of 2000 pct was attained at a temperature of 450 °C and an initial strain rate of $5.6 \times 10^{-2}\ s^{-1}$ with the corresponding strain rate sensitivity coefficient of 0.46. An increase in temperature from 250 °C to 500 °C resulted in a shift of the optimal strain rate for superplasticity, at which highest ductility appeared, to higher strain rates. Superior superplastic properties of the commercial Al-Mg-Sc alloy are attributed to high stability of ultrafine grain structure under static annealing and superplastic deformation at $T \leq 450$ °C. Two different fracture mechanisms were revealed. At temperatures higher than 300 °C or strain rates less than $10^{-1}\ s^{-1}$, failure took place in a brittle manner almost without necking, and cavitation played a major role in the failure. In contrast, at low temperatures or high strain rates, fracture occurred in a ductile manner by localized necking. The results suggest that the development of ultrafine-grained structure in the commercial Al-Mg-Sc alloy enables superplastic deformation at high strain rates and low temperatures, making the process of superplastic forming commercially attractive for the fabrication of high-volume components.

I. INTRODUCTION

THE aerospace industry has a great interest in developing new aluminum alloys with enhanced service properties. Wrought non-heat-treatable Al-Mg alloys containing Sc are attractive candidates for different structural components due to their good weldability, strength, excellent corrosion resistance, and ductility.[1] The fabrication of complex-shaped parts for aerospace structures requires an enhanced workability. It is possible to highly improve the formability of Al-Mg-Sc alloys by making these materials superplastic.[2] Recently, it was established that the best way to achieve high superplastic ductilities in Al-Mg-Sc alloys is an extensive grain refinement by imposing an intense plastic strain (IPS) through a process such as equal-channel angular extrusion (ECAE). Numerous works reported a superior ductility in Al-Mg-Sc alloys, with moderate concentrations of Mg ($\leq$3 pct), subjected to ECAE at exceptionally high strain rates ($\geq 10^{-2}\ s^{-1}$), which makes the process of superplastic forming highly attractive for commercial applications.[3–6] However, commercial Al-Mg-Sc alloys with Mg content less than 4.5 pct exhibit a relatively low strength; therefore, their commercial application is restricted to very specific areas.[1] An attempt by the authors of Reference 4 to make the Al-5 pct Mg-0.2 pct Sc alloy superplastic through ECAE at room temperature was unsuccessful due to the cracking of the samples. Therefore, a different procedure of the ECAE should be applied to produce submicrometer grains in the Al-Mg-Sc alloys containing >3 pct Mg.

Nowadays, among the alloys of the Al-Mg-Sc system, the most attractive material for aerospace applications is the alloy Al-6 pct Mg-0.3 pct Sc, designated in the Former Soviet Union as 1570 aluminum alloy[1] and denoted as 1570 Al herein. The 1570 Al exhibits the highest strength attained in non-heat-treatable commercial aluminum alloys[1] due to an increased content of Mg (~6 pct) and Sc additions. Recent experiments showed that the highest elongation to failure of about 1000 pct at high strain rates $\geq 10^{-2}\ s^{-1}$ was achieved in sheets of the 1570 Al subjected to extensive cold rolling.[7] It was found that the 1570 Al exhibited high superplastic properties in the unrecrystallized condition at temperatures over 450 °C[7] due to the occurrence of continuous dynamic recrystallization during superplastic deformation, which is typical for Al-Mg alloy.[8–11]

The present study was initiated in order to evaluate, in detail, the superplastic behavior at high temperatures and to study the low-temperature limit for high-strain-rate superplasticity in the commercial 1570 Al subjected to ECAE at an elevated temperature. A specific objective of this work is to examine the microstructural evolution, cavitation, and fracture caused by high-strain-rate superplastic deformation.

II. MATERIAL AND EXPERIMENTAL PROCEDURE

The 1570 Al with a chemical composition of Al-5.76 pct Mg-0.32 pct Sc-0.3 pct Mn-0.2 pct Si-0.1 pct Fe (in wt) was manufactured by direct chill casting followed by a solution

F. MUSIN, Senior Research Associate, and R. KAIBYSHEV, Head of Laboratory, are with the Institute for Metals Superplasticity Problems, Russian Academy of Sciences, Khalturina 39, Ufa 450001, Russia. Contact e-mail: rustam@anrb.ru Y. MOTOHASHI, Professor, Research Center for Superplasticity, and G. ITOH, Associate Professor, Department of Mechanical Engineering, are with Ibaraki University, Hitachi 316-8511, Japan.

treatment at 520 °C for 24 hours. The alloy was cut into cylinders of 20 mm in diameter and 100 mm in length. The ECAE was conducted using an isothermal die with a circular internal cross section with the diameter of 20 mm. The channel had an L-shaped configuration with an angle equal to 90 deg. Deformation through this angle produces a strain of approximately 1 on each passage through the die. The pressing speed was approximately 10 mm/s. The rods were repetitively pressed through the dies at 325 °C to a total strain of ~16, and the samples were rotated by 90 deg in the same sense between each pressing (*i.e.*, route B_c[12]).

Tensile specimens were cut parallel to the longitudinal axis of the pressed rods with a gage length of 6 mm and cross section of 1.5 × 3 mm^2. These samples were pulled to failure in air using a Shimadzu* machine (model AG-G-20kN),

*Shimadzu is a trademark of Shimadzu Corporation, Kyoto, Japan.

which operates at a constant crosshead speed. Tension tests were carried out in the temperature interval 250 °C to 500 °C at strain rates ranging from 1.4×10^{-5} to 1.4 s^{-1}. Temperature accuracy was within ±2 °C. Each sample was held at a testing temperature for about 30 minutes in order to reach a thermal equilibrium. The values of the strain rate sensitivity ($m = a \ln \sigma / d \ln \dot{\varepsilon}$, where σ is the flow stress and $\dot{\varepsilon}$ is the strain rate) were determined by strain-rate-jump tests.[13,14] The magnitudes of the elongation to failure were measured by using two scratches marked on the gage section of each sample.

Metallographic analysis was carried out using an Olympus*

*Olympus is a trademark of Olympus Optical Co., Ltd., Tokyo, Japan.

BX60 optical microscope and a JEOL* JSM-840 scanning

*JEOL is a trademark of Japan Electron Optics Ltd., Tokyo.

electron microscope (SEM). A JEOL JEM-2000EX electron microscope with a double-tilt stage at an accelerating voltage of 200 kV was used for the thin foil examinations. Microstructures were analyzed in the sections taken from the planes containing the longitudinal (tension) and long transverse directions. Samples for microstructure examinations were annealed at 170 °C for 4 hours in order to decorate grain boundaries with secondary phase particles. These grain-boundary particles were revealed by etching with a standard Keller's reagent. The mean grain size was determined by the linear intersect method from the measurements of more than 300 grains. Cavitation was measured in samples pulled to failure by optical microscopy using the standard point-count technique. Areas located 1, 5, and 10 mm apart from the fracture surface were analyzed. Misorientations of (sub) grain boundaries were studied by electron backscattering diffraction (EBSD) analysis using a JEOL JSM-840 SEM fitted with an automated EBSD pattern collection system provided by Oxford Instruments, Ltd.

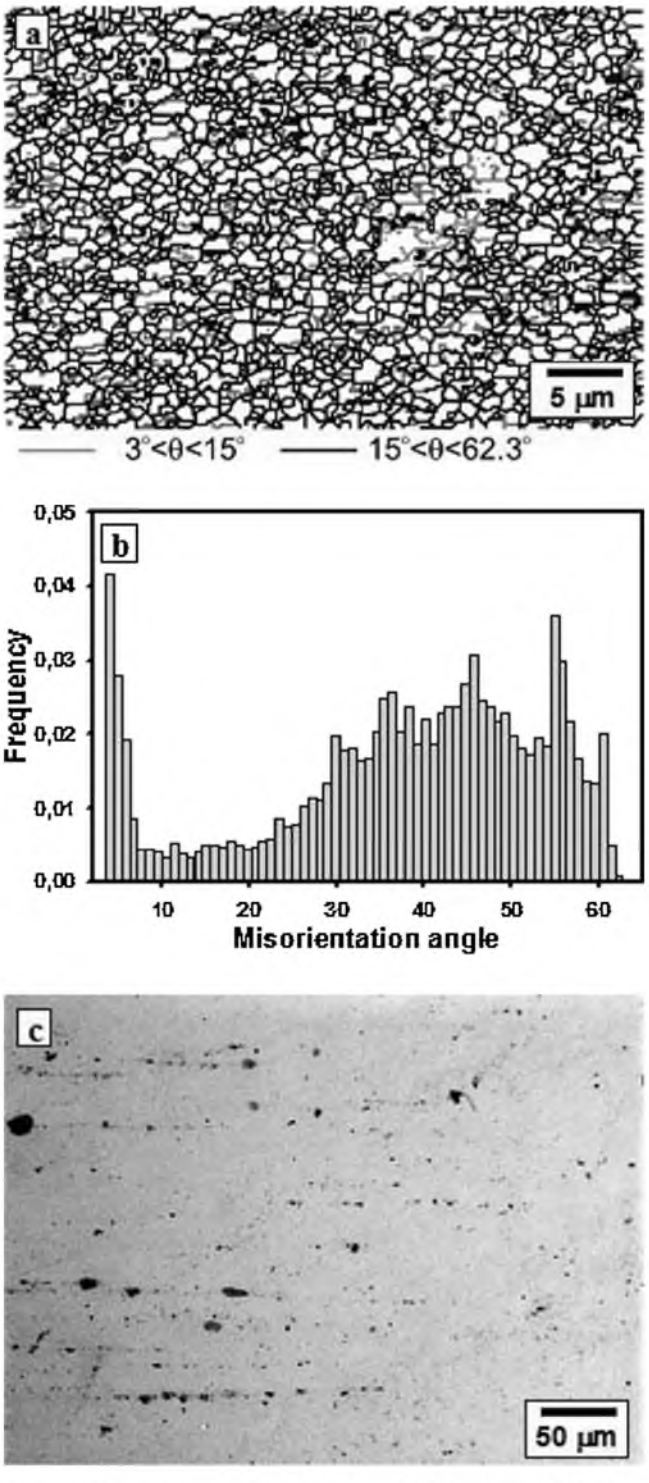

Fig. 1—Microstructure of the 1570 Al subjected to ECAE at 325 °C to a total strain of 16: (*a*) EBSD map, (*b*) misorientation distribution, and (*c*) unetched polished surface. Note that the extrusion axis is horizontal.

III. RESULTS

A. *Microstructure after ECAE*

The microstructure of the 1570 Al after solution treatment consisted of coarse grains with an average size of about 200 μm. Second-phase particles were identified by the TEM analysis as Al_2FeSi and Al_3Sc. The ECAE resulted in uniform microstructure with an average grain size of 1 μm (Figure 1(a)). A careful examination of many areas showed that the microstructure of the ECAE-processed 1570 Al is reasonably homogeneous on the macroscopic level, although elongated areas containing recovered subgrains were rarely observed. The volume fraction of unrecrystallized areas was about 5 pct.

It was shown that about 80 pct of grain boundaries were high-angle boundaries with misorientations over 15 deg (Figure 1(b)). Chains of secondary phase particles, mainly of Al_2FeSi aligned along the prior extrusion direction, were revealed on the unetched surface as stringers of dark pits (Figure 1(c)).

B. *Mechanical Properties*

The typical true stress *vs* true strain (σ-ε) curves for the 1570 Al subjected to ECAE at initial strain rates ranging from 1.4×10^{-4} to 1.4 s^{-1} in the temperature interval 250 °C to 500 °C are shown in Figure 2. It is seen that both the temperature and the strain rate affect the shape of the σ-ε curves. At all temperatures and strain rates, extensive strain hardening takes place initially. After reaching a maximum, the flow stress continuously decreases until failure. An increase in temperature or a decrease in strain rate led to a shift of the peak stress to a higher strain and a reduction in initial work hardening. At $T \geq 300$ °C and $\dot{\varepsilon} < 1.4 \times 10^{-1}$ s^{-1}, the peak stress is attained at $\varepsilon \geq 1$. The stage of strain softening is short; softening is observed only just before the failure. As a result, very uniform deformation visible within the gage lengths was found; the samples exhibit superior tensile ductilities. In contrast, at $T < 300$ °C or $\dot{\varepsilon} \geq 1.4 \times 10^{-1}$ s^{-1}, the peak stress is reached at $\varepsilon \leq 0.25$; a sharp softening after the peak stress can be attributed to extensive localization of plastic flow resulting in the final necking. Subsequent fracture occurs due to well-defined unstable plastic flow. Steady-state flow was not found at all examined temperatures despite the fact that the value of elongation to failure is high. It should be noted that such a variation of the flow stress with strain is not typical for conventional superplastic materials, in which the flow stress is almost independent of strain.[13,14] It is necessary to emphasize that the most important mechanical characteristic of ECAE-processed 1570 Al is extensive strain hardening at strains less than the peak strain, ε_p, at which the peak stress appears.

The relationship between the peak stress, σ_p, and the peak strain, ε_p, is plotted in Figure 3. It is seen that the ε_p value tends to increase gradually with the decreasing peak stress. In general, an increase in temperature or a decrease in strain rate results in an increase in the ε_p value. It is worth noting that the highest values of elongation to failure (≥1000 pct) were attained at temperatures and strain rates at which the peak strain usually is higher than 1.0. Thus, high values of total elongation correlate with high ε_p values.

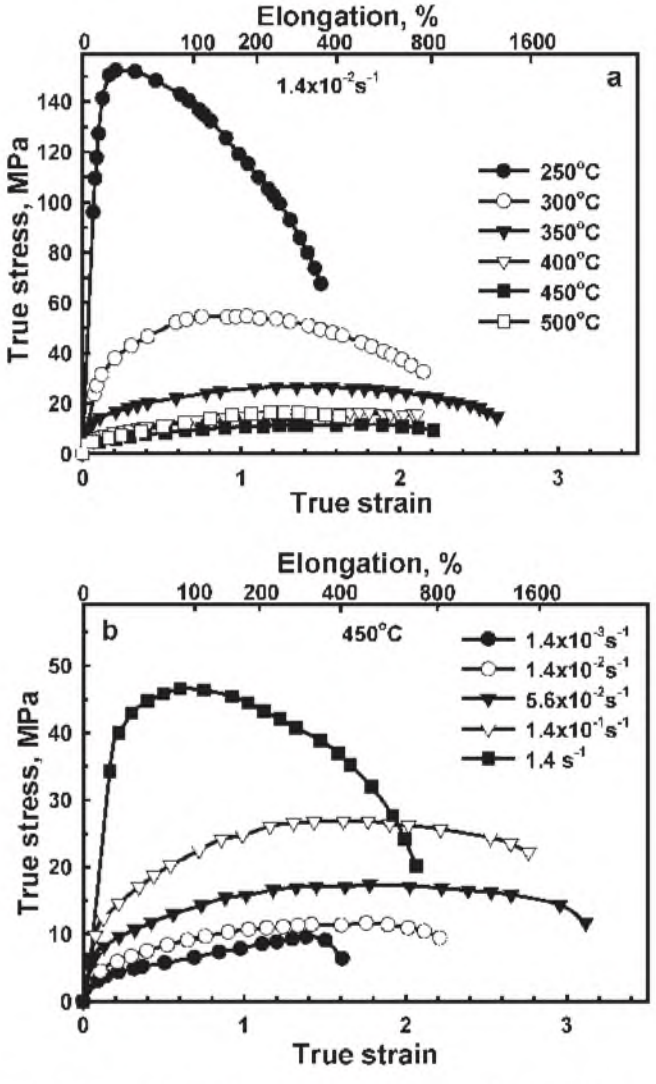

Fig. 2—Effect of (*a*) temperature and (*b*) strain rate on the true stress–true strain curves for the ECAE-processed 1570 Al.

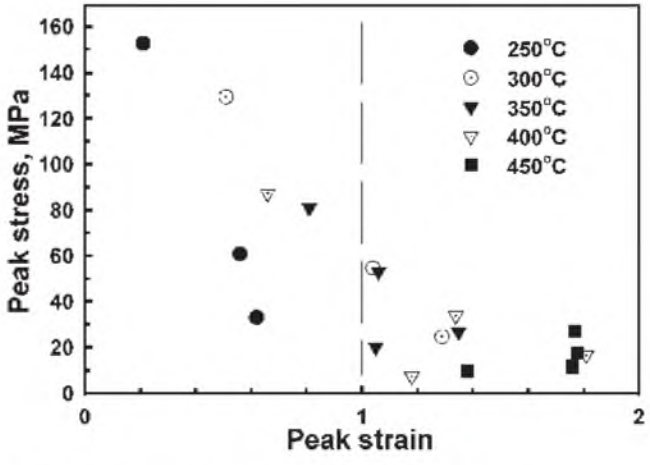

Fig. 3—Relationship between peak strain and peak stress.

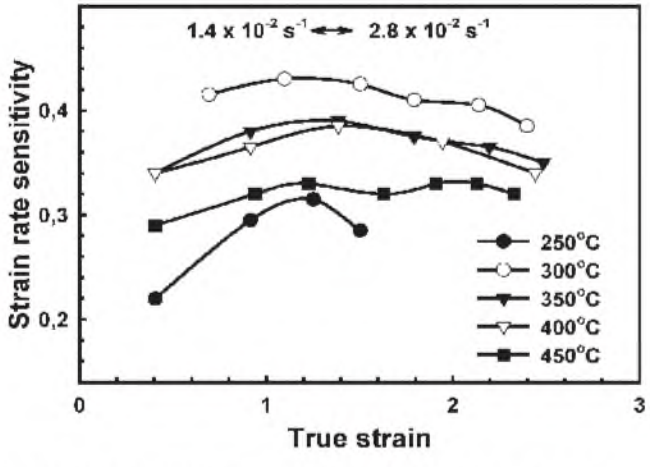

Fig. 4—The effect of true strain on the coefficient of strain rate sensitivity.

The coefficient of the strain rate sensitivity, m, as a function of true strain is shown in Figure 4. It is seen that at $T \geq 300$ °C and $\dot{\varepsilon} = 1.4 \times 10^{-2}$ s^{-1}, a weak strain dependence of the m value appears. The m value is higher than 0.33 at all strains and slightly increases at strains less than the peak strain. Subsequent deformation results in a gradual decrease in the m value. At 250 °C, increasing strain leads to an increase in the m value from 0.22 to 0.32 followed by a decrease in the m value.

The flow stress taken at a true strain of 0.4 as a function of the initial strain rate is plotted on a double logarithmic scale in Figure 5(a). The variations of strain rate sensitivity, m, and elongation to failure, δ, with strain rate are shown in Figures 5(b) and (c). The σ-$\dot{\varepsilon}$ curves show evidence of a sigmoidal shape, indicating three well-known regions of superplastic deformation[13,14,15] at all temperatures examined. Elongation to failure and the strain rate sensitivity coefficient are found to have a maximum in region 2 (in which $m \geq 0.33$) and tend to decrease on either side of the strain rate associated with these maximum values. It is seen that increasing temperature results in decreasing flow stress and shifting the optimal strain rate region for superplasticity (region 2) to higher strain rates. At 250 °C, the highest elongation to failure of 550 pct appears at a strain rate of 1.4×10^{-3} s^{-1} at which the highest m value of 0.36 was found. A temperature increase from 250 °C to 300 °C results in a shift of the optimal strain rate for superplasticity, at which the highest elongation to failure is attained, from $\sim 1.4 \times 10^{-3}$ to $\sim 1.4 \times 10^{-2}$ s^{-1}, and an increase in the maximum m value from 0.36 to 0.44. In the temperature interval 300 °C to 400 °C, the highest ductilities are observed at lower strain rates compared with those at which the highest m values appear. It is worth noting that at these temperatures, the highest δ value tends to increase with increasing temperature despite the fact that the highest m value ~ 0.44 remains essentially unchanged. At 450 °C, a continuous increase in the m value with increasing strain rate was revealed in the examined strain rate range despite the fact that a well-defined maximum of elongation to failure was found at an initial strain rate of 5.6×10^{-2} s^{-1}. It is apparent that, at 450 °C, the strain rate, at which the highest m value appears, was so high that it has not been achieved in the present study.

To evaluate the reproducibility of experimental data, at least three samples for each testing temperature were pulled to failure at an initial strain rate of 1.4×10^{-2} s^{-1} in the temperature range 250 °C to 500 °C (Figure 6). It is seen that the ECAE-processed 1570 Al exhibits ductility higher than 400 pct at all temperatures examined. In the temperature range of 300 °C to 450 °C, the ductility of all ECAE-processed samples was higher than 800 pct. Thus, the 1570 Al subjected to ECAE shows superior superplastic properties, which are suitable for commercial applications.

C. *Microstructural Evolution*

The microstructural evolution of the 1570 Al was examined under conditions of static annealing in grip sections and

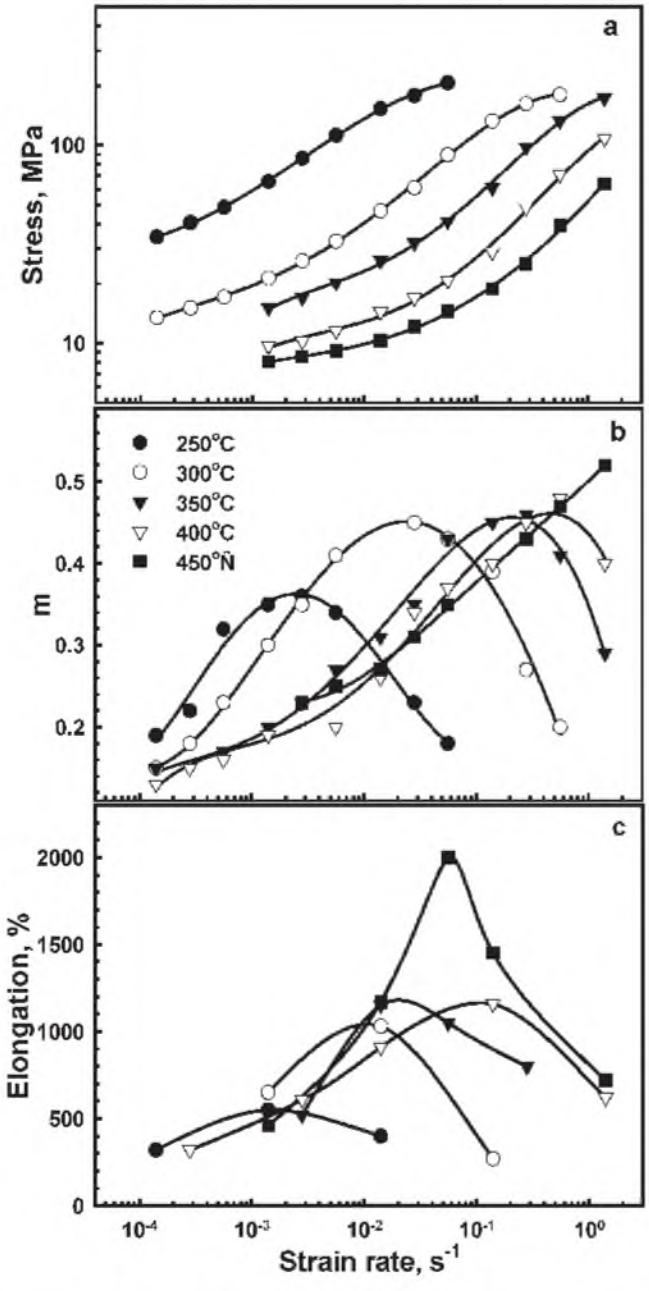

Fig. 5—The variation of (*a*) flow stress (*b*) strain-rate-sensitivity coefficient, m, and (*c*) elongation to failure with strain rate.

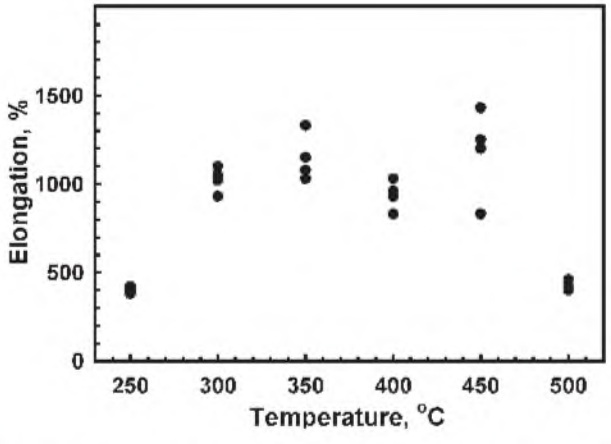

Fig. 6—Temperature dependencies of the elongation to failure at an initial strain rate of 1.4×10^{-2} s^{-1}.

during superplastic deformation, *i.e.*, dynamic annealing, in the gage section at initial strain rate of 1.4×10^{-2} s^{-1} in the temperature range of 250 °C to 500 °C (Figure 7). Grain sizes observed after the static and dynamic annealing and grain aspect ratio (AR), defined as the ratio of the grain dimension in the longitudinal direction to that in the transverse direction, are summarized in Table I. It is seen that in the 1570 Al, the ultrafine grains produced by ECAE processing exhibit a superior stability under static annealing. Increasing temperature from 250 °C to 450 °C leads to a static growth of grains from 1 to 1.9 μm (Table I, Figure 7(a)).

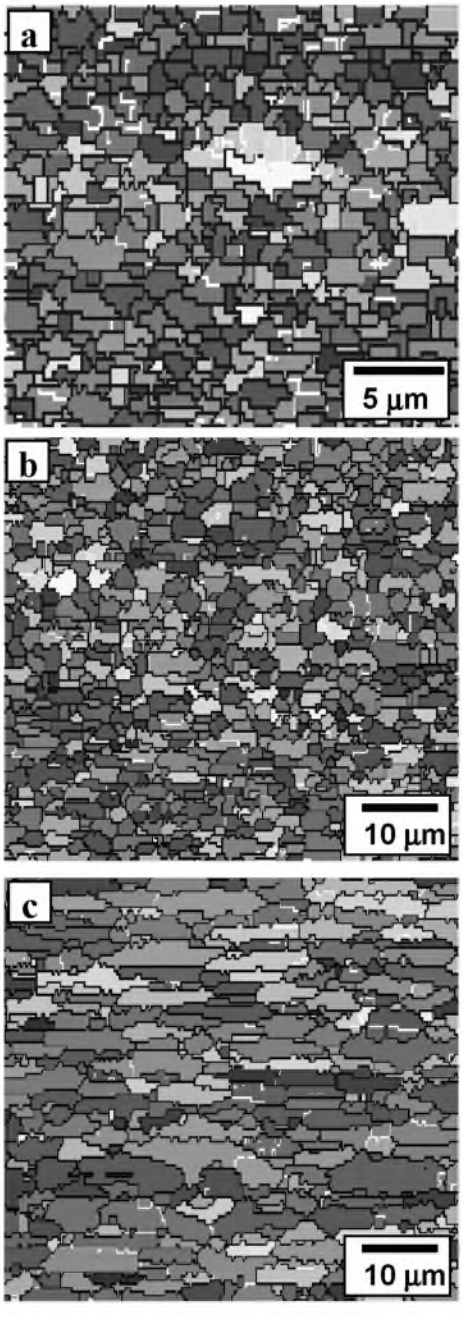

Fig. 7—EBSD maps of the 1570Al: (*a*) grip section at 450 °C, (*b*) gage section at 300 °C and 1.4×10^{-2} s^{-1}, and (*c*) gage section at 450 °C and 5.6×10^{-2} s^{-1}. Note that the tension axis is horizontal.

At T > 450 °C, onset of extensive grain growth was detected in the grip section.

Superplastic deformation leads to a remarkable strain-induced grain growth. However, the grain size remains on average less than 4 μm even after 2000 pct elongation at 450 °C and 5.6×10^{-2} s^{-1} (Figure 7(c)). No extensive elongation of initial grains along the tension axis was found (Table I). The values of AR are typical for conventional superplastic alloys, where a high contribution of grain boundary sliding (GBS) to the total elongation takes place.[13,14] Notably, in samples exhibiting lower ductility, the AR is higher. It is well known that high values of AR are indicative of an increased contribution of dislocation glide to the total deformation. At 500 °C, concurrent grain growth is expected to reduce the likelihood of GBS resulting in a reduced ductility. It is worth noting that the superplastic deformation produces essentially similar grain sizes in both states of the 1570 Al subjected to ECAE processing and extensive cold rolling.[7]

D. *Cavitation and Fracture*

Cavitation during superplastic deformation of the 1570 Al was examined in the samples pulled to failure at various strain rates and temperatures (Table II). Typical examples of cross-sectional views of the specimens pulled to failure at a strain rate of 1.4×10^{-2} s^{-1} are shown in Figure 8.

At $T < 300$ °C, the superplastic deformation induces a limited cavitation. It is pointed out that most of the dark phases in Figure 8(a) might be, in fact, impurity inclusions. The cavities and secondary phase particles form short stringers elongated along the tension direction. No cavities located outside these stringers were found. With increasing temperature, the volume fraction of the pores strongly increases and approaches a value of about 13.3 pct at 450 °C (Table II, where the data for areas located at position 1 mm from the fracture surface are presented). At $T > 300$ °C, two types of cavities are formed during superplastic deformation (Figure 8(b)). Cavities with sizes ranging from 0.2 to 0.5 μm belong to the voids of the first type. These cavities are randomly distributed within the volume of material and have an equiaxed shape, suggesting a diffusion-controlled cavity growth.[13,15] Notably, the volume fraction of these cavities is significantly less than 1 pct even at $T \geq 450$ °C and low strain rates. It is apparent that the nucleation and growth of these voids could not result in the material failure.

Cavities belonging to the second type have a jagged shape, suggesting a plasticity-controlled cavity growth mechanism.[13,15] These voids locate near coarse Al_2FeSi inclusions, forming stringers along the tension direction (Figures 8(b) and (c)). This type of cavitation results in the pseudo-brittle fracture of the 1570 Al at $T > 300$ °C. It is known[13] that such cavities nucleate at hard particle/metal interfaces. This is attributed to the limited ability of the Al_2FeSi phase to contribute to the accommodation of GBS. Therefore, the Al_2FeSi phase appears to be largely responsible for the cavitation in the 1570 Al. It is in contrast with high-purity Al-Mg-Sc alloys in which the cavitation plays an unimportant role in failure.[3–6] Therefore, it can be expected that the 1570 Al containing a reduced amount of Fe and Si can exhibit an enhanced ductility.

The effect of the strain rate on volume fraction of porosity for two temperatures of 300 °C and 400 °C is shown in

Table I. Average Grain Sizes after Static Annealing, L_S, and Superplastic Deformation, L_D, and the Grain Aspect Ratio (AR) for the Samples Pulled to Failure at Different Temperatures; the True Strain in the Gage Section and the Time of Static Annealing in the Grip Section (in Hours) Are Also Indicated

T, °C	250 0.58 h, 380 Pct	300 0.72 h, 1100 Pct	350 0.77 h, 1330 Pct	400 0.69 h, 930 Pct	450 0.67 h, 830 Pct	500 0.59 h, 410 Pct
L_S, μm	1.0	1.0	1.2	1.3	1.9	7.4
L_D, μm*	1.6/1.4	1.6/1.3	1.9/1.4	3.1/2.0	5.8/3.1	7.1/4.3
AR	1.14	1.23	1.36	1.55	1.87	1.65

*Numerator and denominator are grain sizes measured in the longitudinal and transverse directions, respectively.

Table II. Volume Fraction of Cavities, V, for the Samples Pulled to Failure at a Strain Rate of $1.4 \times 10^{-2}\ s^{-1}$ and Different Temperatures; Areas Located 1, 5, and 10 mm from the Fracture Surface Were Analyzed

T, °C	250 420 Pct	300 1100 Pct	350 1330 Pct	400 930 Pct	450 830 Pct	500 410 Pct
V_{1mm}, pct	0.14	2.3	5.2	4.9	13.2	11.4
V_{5mm}, pct	0.1	0.6	2.1	2.0	5.3	6.7
V_{10mm}, pct	0.0	0.1	0.53	0.13	1.2	4.0

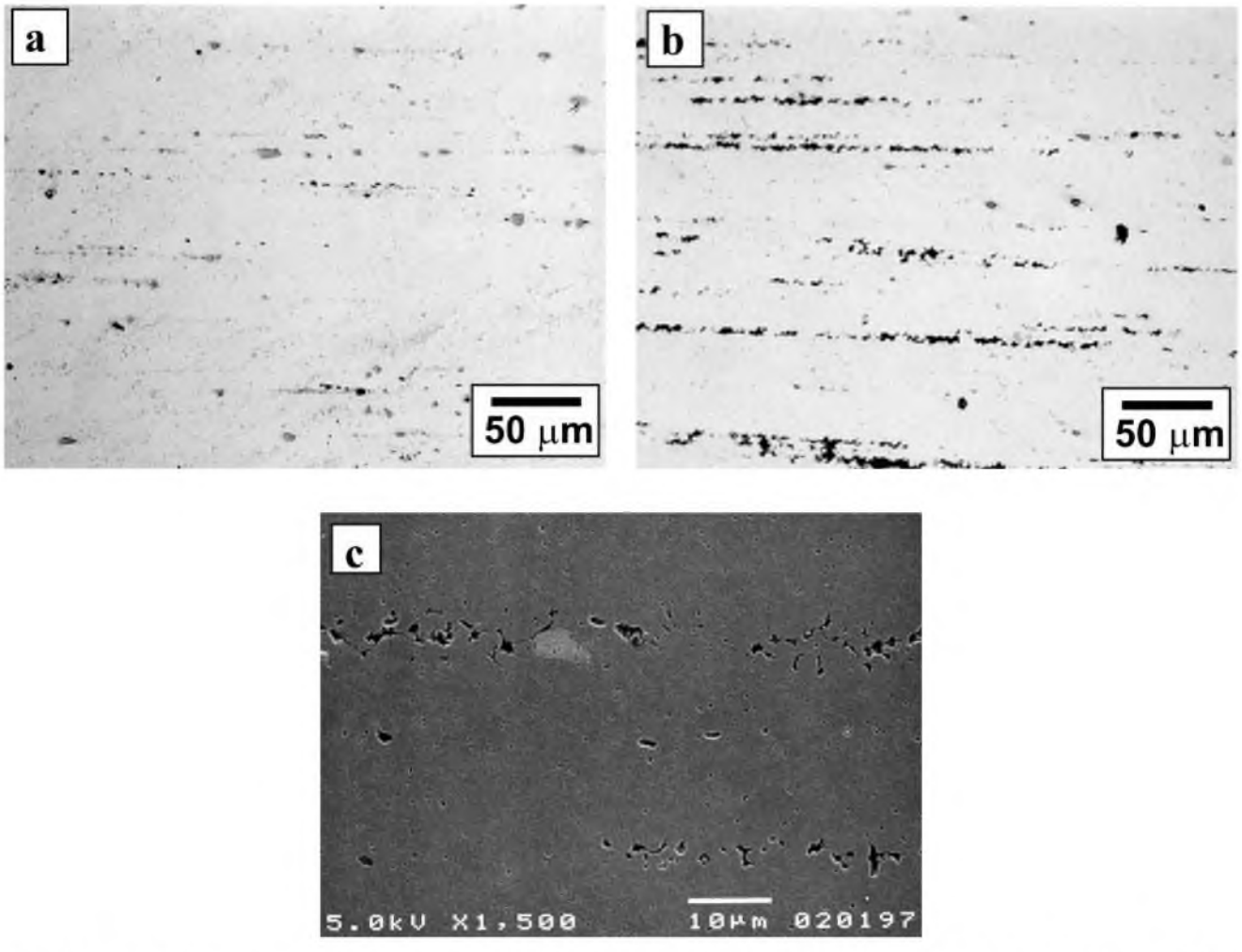

Fig. 8—Cross-sectional view of samples strained at $\dot{\varepsilon} = 1.4 \times 10^{-2}\ s^{-1}$. Micrographs were taken in places 5 mm from the fracture surface: (*a*) 250 °C, and (*b*) and (*c*) 350 °C. Note that the tension axis is horizontal.

Figure 9. At 300 °C, the porosity was found to have a maximum at a strain rate of 1.4×10^{-3} s^{-1} and tended to decrease on either side of the strain rate associated with this highest value. An increase in temperature leads to a shift of the maximum of the porosity volume fraction toward higher strain rates.

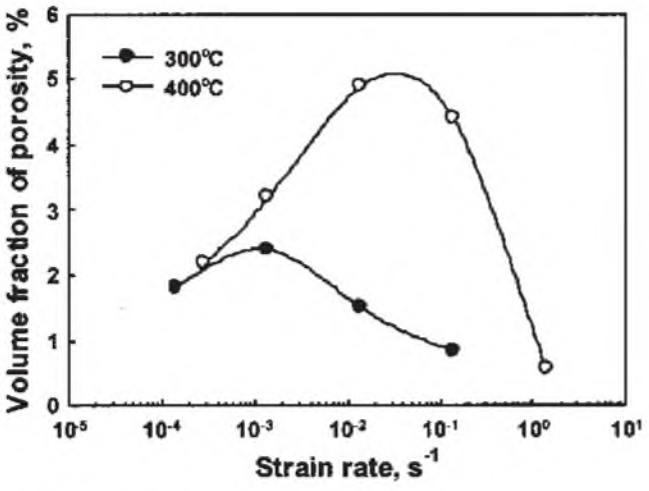

Fig. 9—The effect of strain rate on the volume fraction of porosity. Areas located at a position about 1 mm from the fracture surface were analyzed.

Cross-sectional views of near-fracture-surface regions of the samples strained to failure are shown in Figure 10. It is seen that two types of fracture are distinctly distinguished. At temperatures higher than 300 °C or strain rates less than 10^{-1} s^{-1}, the fracture occurs abruptly in a brittle manner almost without necking (Figures 10(a) and (b)), suggesting that the cavitation plays a major role in the failure. The formation of bridges between the free surfaces and cavity stringers located near them (Figure 11(a)) as well as an interlinkage of the cavity stringers in the transverse direction (Figure 11(b)) initiates the pseudo-brittle fracture, which occurs without strain localization. The second type of fracture mechanism is observed at temperatures less than 300 °C or strain rates over 10^{-1} s^{-1}. Under these conditions, the change of the fracture mechanism from the one caused by porosity to the ductile type takes place. The alloy hardly has any cavitation and the samples break down with localized necking (Figures 10(c) and (d)).

It is worth noting that an essentially high amount of cavities formed during deformation does not lead to a drop of superplastic properties. It is evident that an extensive cavitation takes

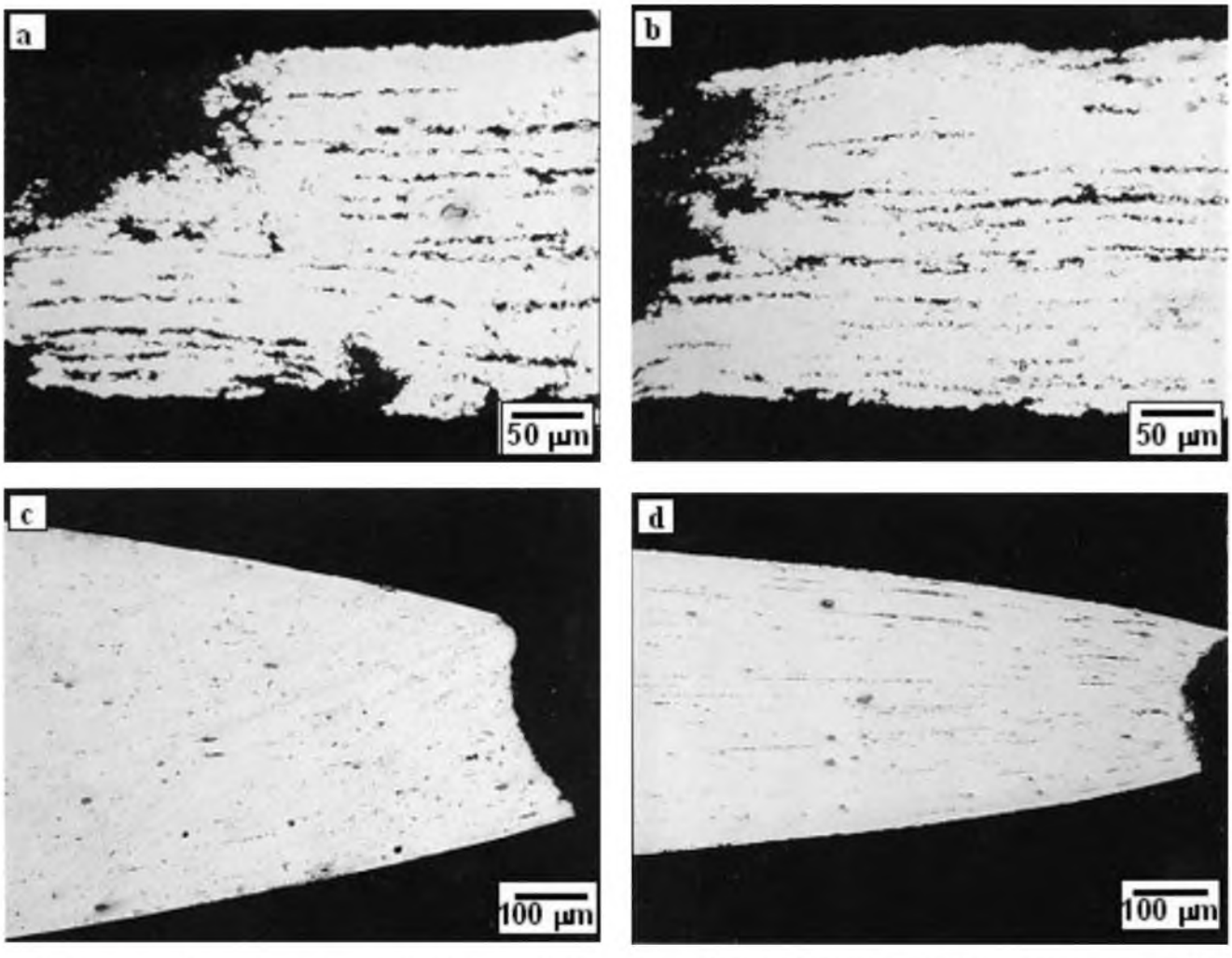

Fig. 10—Cross-sectional views of samples strained to failure near the fracture tip: (*a*) 350 °C, 1.4×10^{-2} s^{-1}; (*b*) 400 °C, 1.4×10^{-1} s^{-1}; (*c*) 250 °C, 1.4×10^{-2} s^{-1}; and (*d*) 400 °C, 1.4×10^{0} s^{-1}.

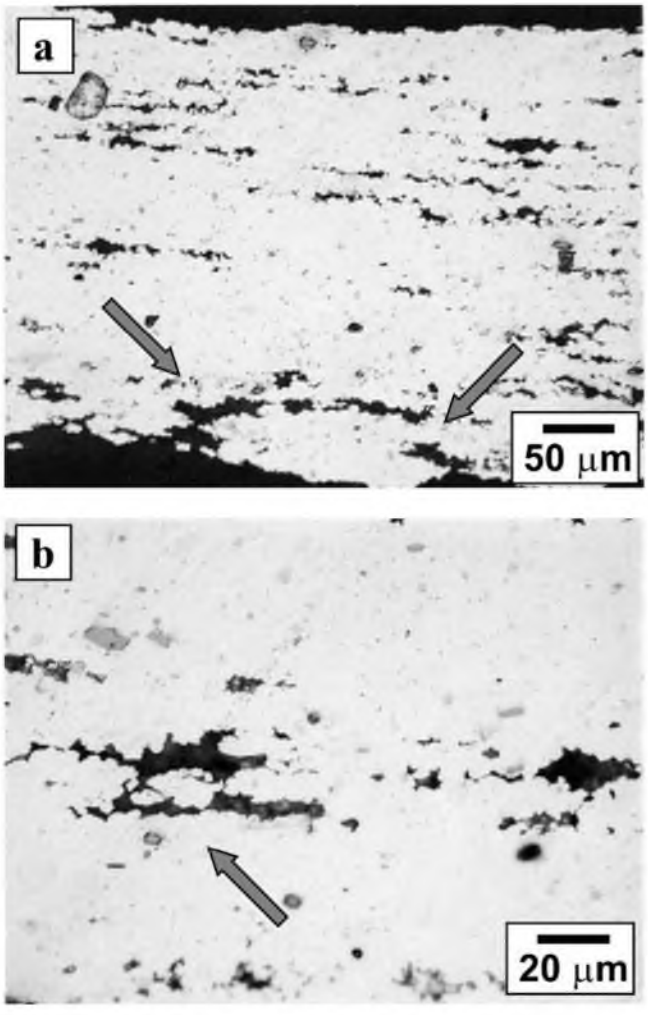

Fig. 11—Cross-sectional view of samples strained at 400 °C and $\dot{\varepsilon} = 1.4 \times 10^{-2}\ s^{-1}$. Micrographs were taken 1 mm from the fracture surface.

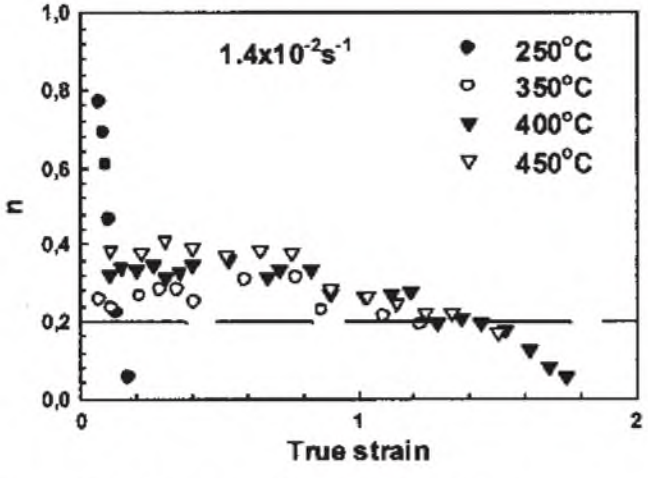

Fig. 12—Effect of true strain on the strain-hardening coefficient, *n*.

place only on the later stages of superplastic deformation, because the amount of the cavities quickly decreases with the distance from the fracture surface (Table II).

IV. DISCUSSION

A. *Microstructural Aspects of Superplasticity*

The present study demonstrated that the ECAE at 325 °C to a strain of 16 is an attractive way to produce fully recrystallized structure with the grain size of about 1 μm in the 1570 Al. It is well known that the strain rate in superplasticity, $\dot{\varepsilon}$, generally obeys the following relationship:[13]

$$\dot{\varepsilon} = A\frac{DG\mathbf{b}}{kT}\left(\frac{\mathbf{b}}{d}\right)^{p}\left(\frac{\sigma}{G}\right)^{2} \qquad [1]$$

where A is a dimensionless constant, $\mathbf{b}$ is the Burgers vector, d is the grain size, σ is the applied stress, G is the shear modulus, k is the Boltzmann's constant, D is the grain boundary diffusion coefficient and defines the temperature dependence of the strain rate at constant stress and structure, T is the absolute temperature, and p is the exponent of the inverse grain size ranging from 2 to 3. The grain size in 1570 Al after ECAE at $T = 325$ °C is about 5 times larger than that in the Al-3 pct Mg-0.2 pct Sc alloy after ECAE at room temperature.[3–6] Hence, one can expect that a superplastic ductility in the Al-3 pct Mg-0.2 pct Sc alloy can be achieved at a significantly higher strain rate than that in the 1570 Al. However, a careful inspection of the data reported in previous works[3–6] and obtained in the present study shows that the optimal strain rate for superplasticity of the Al-3 pct Mg-0.2 pct Sc alloy is essentially the same or even less than that for the 1570 Al. This can be caused by the fact that the starting grain size of 0.2 μm in the Al-3 pct Mg-0.2 pct Sc alloy is unstable under the dynamic annealing conditions[4] and the resulting grain size, d, in Eq. [1] will be essentially the same for both materials at $T \geq 350$ °C. It is worth noting that in the temperature range 250 °C to 300 °C, where grain size of the Al-3Mg-0.2Sc alloy after static annealing is less by a factor of 2 than that in the 1570 Al, the highest elongation to failure and the optimal strain rate for superplasticity are almost the same for both materials.[6] At 450 °C, the grain size in the Al-3Mg-0.2Sc alloy is the same as that in the 1570 Al. At this temperature, the Al-3Mg-0.2 Sc alloy exhibits ductilities of 660 and 130 pct at strain rates of 10^{-1} and $10^{0}\ s^{-1}$, respectively, whereas the ductilities of the 1570 Al at the same strain rates are 1450 and 780 pct. Thus, the achievement of a finer grain size in Al-Mg-Sc alloy through the IPS at room temperature has no advantages as compared to the production of micrometer scale grains through an ECAE at intermediate temperatures, because the grain size resulting from superplasticity at optimal conditions will be essentially the same. Therefore, the IPS at an elevated temperature (325 °C) is highly suitable for the development of superplasticity in Al-Mg-Sc alloys because of their enhanced workability at these conditions.

B. *Superplastic Behavior in Recrystallized Condition*

Analysis of the data reported in the present article shows that the 1570 Al with a fully recrystallized structure with a mean grain size of about 1 μm is a material exhibiting high-strain-rate-superplasticity with superior ductilities (>1000 pct) in the temperature interval 300 °C to 450 °C and low-temperature superplasticity with a moderate elon-

gation to failure of 550 pct at 250 °C. Superplastic behavior of the 1570 Al with a recrystallized microstructure is distinctly different from that of this alloy with a starting unrecrystallized structure[7] and is not typical for conventional superplastic materials.[13] The difference in the highest tensile elongations of the 1570 Al in two structural conditions with the unrecrystallized initial structure[7] and the fully recrystallized structure is not too large due to the fact that superplastic deformation results in similar grain size. However, the ECAE processing leads to a significant expansion of the temperature–strain rate domain of superplastic deformation and allows achieving high ductilities both at higher strain rates and lower temperatures.

The 1570 Al subjected to ECAE exhibits a wide strain interval, in which an extensive strain-hardening occurs. This is the main feature of the superplastic behavior of the fine-grained 1570 Al with a fully recrystallized structure. An increase in the flow stress with strain is normally indicative of strain-enhanced grain growth.[13] However, in the 1570 Al, the increasing coefficient of strain rate sensitivity is associated with the strain hardening stage. It is well known that dynamic grain growth during superplastic deformation leads to a reduction in the strain rate sensitivity with increasing strain.[13,14,15] In addition, the rate of strain hardening is higher at low temperatures and high strain rates at which no remarkable grain growth was found. Therefore, strain hardening at the initial stage of superplastic deformation in the 1570 Al is not attributed to dynamic grain growth and can be caused by a peculiarity of the GBS, which was considered in Reference 16.

At $T \leq 300$ °C or $\dot{\varepsilon} \geq 1.4 \times 10^{-1}$ s^{-1}, apparent strain softening is attributed to extensive necking and strain localization. At higher temperatures and lower strain rates, marginal strain softening after the peak stress can be associated with the development of cavitation damage.

C. *Stability of Superplastic Flow*

It is known[13–15,17] that the fracture of superplastic materials during tensile deformation results from an unstable plastic flow or cavitation. A high value of the strain rate sensitivity coefficient ($m \sim 0.5$) confers a high resistance to the neck development and results in a high tensile elongation in conventional superplastic aluminum alloys.[13,14,15] However, the present 1570 Al demonstrates superior ductilities corresponding to moderate values of m (≤0.4). It is well known that the plastic stability in tension is maintained, if the sum n + m, where n is the strain-hardening coefficient and m is the coefficient of strain rate sensitivity defined by the equation[13]

$$\sigma = K \dot{\varepsilon}^m \varepsilon^n \qquad [2]$$

where K is a constant, is high. The presence of a neck in a material under tension leads to locally high strain rate and increased strain. As a result, for high values of m and n, a sharp increase in the flow stress within the necked region occurs, providing a resistance to further neck growth. It was demonstrated[13,14] that if $n + m > 0.5$, the fracture does not occur due to unstable plastic flow. In classic superplastic material, the n value is almost zero; the plastic stability is mainly provided by high values of m.[13]

Typical dependence of the strain exponent, n, against true strain, ε for the 1570 Al subjected to ECAE is presented in Figure 12. In condition of low-temperature superplasticity ($T < 300$ °C), a stable plastic flow occurs only at strains less than the peak strain, ε_p due to high value of the strain-hardening coefficient. After reaching the peak strain, the $m \leq 0.36$ value is not enough to inhibit neck development; unstable plastic flow results in material fracture. Therefore, 1570 Al exhibits moderate superplastic properties at low temperatures.

Under the condition of high-strain-rate superplasticity at $T > 300$ °C, the sum $n + m$ has values larger than 0.5, thus providing a stable plastic flow. At these conditions, the ε_p value is not less than 1, and therefore, superior stability of superplastic flow associated with high strain hardening takes place in a wide strain range. As a result, the 1570 Al exhibits very high superplastic ductilities (≥800 pct) despite the fact that the m value ranges from 0.33 to 0.46. In conventional superplastic materials, where strain hardening is almost zero, the elongations to failure usually do not exceed 600 pct if the m values are less than 0.4.[13] Thus, the high superplastic ductilities of the 1570 Al with fine-grained structure at high strain rates are associated with the high magnitude of the strain-hardening coefficient.

V. CONCLUSIONS

1. It was found that ECAE processing at 325 °C to a true strain of 16 provides a formation of a uniform structure with an average grain size of about 1 μm in the 1570 aluminum alloy. This ultrafine grain size was essentially stable at elevated temperatures under both the static annealing and superplastic deformation.
2. The ECAE-processed 1570 Al exhibits high-strain-rate superplasticity. High tensile elongations (>1000 pct) were found at temperatures ranging from 300 °C to 450 °C and strain rates ranging from 1.4×10^{-2} to 1.4×10^{-1} s^{-1}. The highest elongation to failure of 2000 pct with the corresponding strain-rate-sensitivity coefficient of 0.46 was recorded at 450 °C and an initial strain rate of 5.6×10^{-2} s^{-1}.
3. The ECAE-processed 1570 Al exhibits superplasticity at low temperatures. At 250 °C and an initial strain rate of 1.4×10^{-3} s^{-1}, the highest elongation to failure is 550 pct with corresponding strain-rate-sensitivity coefficient of 0.36.
4. Two different fracture mechanisms in ECAE-processed 1570 Al were revealed at high-strain-rate superplasticity. At temperatures higher than 300 °C or strain rates less than 10^{-1} s^{-1}, failure took place in a brittle manner practically without necking as the result of cavitation. On the contrary, at low temperatures or high strain rates, fracture occurred in a ductile manner resulting from localized necking. At these conditions, evidence of a very limited cavitation was found.

ACKNOWLEDGMENTS

This work was supported, in part, by the International Science and Technology Centre under Project No. 2011, Russian Foundation of Basic Research under Grant No. RFBR01-02-04004, German Research Council (DFG) under Grant

No. DFG436 RUS 113/619/0 (R), and Japan Light Metal Educational Foundation.

REFERENCES

1. YA. Filatov, V.I. Yelagin, and V.V. Zakharov: *Mater. Sci. Eng.*, 2000, vol. 280A, pp. 97-101.
2. R.R. Sawtell and C.L. Jensen: *Metall. Trans. A*, 1990, vol. 21A, pp. 421-30.
3. Z. Horita, M. Furukawa, M. Nemoto, A.J. Barnes, and T.G. Langdon: *Acta Mater.*, 2000, vol. 48, pp. 3633-40.
4. M. Furukawa, A. Utsunomiya, K. Matsubara, Z. Horita, and T.G. Langdon: *Acta Mater.*, 2001, vol. 49, pp. 3829-38.
5. S. Lee, A Utsunomiya, H. Akamatsu, K. Naishi, M. Furukawa, Z. Horita, and T.G. Langdon: *Acta Mater.*, 2002, vol. 50, pp. 553-64.
6. S. Komura, Z. Horita, M. Furukawa, M. Nemoto, and T.G. Langdon: *Metall. Mater. Trans. A*, 2001, vol. 32A, pp. 707-16.
7. T.G. Nieh, L.M. Hsiung, J. Wadsworth, and R. Kaibyshev: *Acta Mater.*, 1998, vol. 46, pp. 2789-00.
8. T.R. McNelley, E.-W. Lee, and M.E. Mills: *Metall. Trans. A*, 1986, vol. 17A, pp. 1035-41.
9. S.J. Hales and T.R. McNelley: *Acta Metall.*, 1988, vol. 36, pp. 1229-39.
10. S.J. Hales, T.R. McNelley, and H.J. McQueen: *Metall. Trans.*, 1991, vol. 22A, pp. 1037-47.
11. E.W. Lee and T.R. McNelley: *Mater. Sci. Eng.*, 1987, vol. 93, pp. 45-55.
12. Z. Horita, M. Furukawa, M. Nemoto, and T. G. Langdon: *Mater. Sci. Technol.*, 2000, vol. 16, pp. 1239-45.
13. J. Pilling and N. Ridley: *Superplasticity in Crystaline Solids*, The Institute of Metals, London, 1989, p. 214.
14. O.A. Kaibyshev: *Superplasticity of Alloys, Intermetallides, and Ceramics*, Springer-Verlag, Berlin, 1992, p. 316.
15. T.G. Nieh, J. Wadsworth, and O.D. Sherby: *Superplasticity in Metals and Ceramics*, Cambridge University Press, New York, NY, 1996, p. 210.
16. R. Kaibyshev, F. Musin, D.R. Lesuer, and T.G. Nieh: *Mater. Sci. Eng.*, 2003, vol. A342, pp. 169-77.
17. J.W. Edington, K.N. Melton, and C.P. Cutler: *Progr. Mater. Sci.*, 1976, vol. 21, pp. 161-68.